**Background**

The cervical spine (CS) consists of 7 vertebrae. The C1 and C2 vertebrae, also called the atlas and the axis, are unique in function and shape. The left and right rotation of the neck is mainly responsible C1-C2 vertebrae in the upper part of the cervical spine, and the back-and-forth swing of the neck is performed by the cervical vertebrae between C3-C7 vertebrae in the lower part. To do a surgery in the cervical spine, vertebrae C1 and C2 are very difficult than others (C3-C7) because they are uniquely shaped, the vertebral foramen which allow the vertebral arteries to reach through to the brain and supply it with blood and are only seen in the cervical C1/C2 region. Approximately, 50% of the rotation of the neck happens between C1 and C2 [1].

Common problems of C1-C2 vertebrae include arthritis, fractures, vertebral artery injury, occipital neuralgia, and crowded dense syndrome. The various symptoms of the problems are headache, fatigue, dizziness, and nausea. A fracture of the upper cervical spine in the elderly is a serious injury. Their frequency is rising. Sufficient stability to allow the fracture to heal is very important. C2 fracture is a common injury in elders. Treatment becomes confusing due to osteoporosis and patient comorbidities [2]. From research [3], there is extensive evidence that the recurrence rate of upper spine injuries, especially atlantoaxial fractures, is high in elders due to reduced bone thickness, various injury systems, and degenerative changes affecting spinal biomechanics. Degenerative changes cause stiffening of the CS prompting diminished portability and therefore to a higher frequency of upper CS wounds. Mortality rates as high as 25-30% have been reported after odontoid fractures in elders [4]. One of the most treatment options is spinal fusion surgery with trans articular screw fixation [5].

Instability of the atlantoaxial complex may result from provocative, horrible, innate, neoplastic, or degenerative issues and frequently requires careful stabilization. Beginning dorsal wiring methods permit safe fixation yet require unbending outer immobilization and have been related to high combination disappointment rates. Rigid screw fixation methods include trans articular screw fixation and C1-C2 rod-cantilever fixation to provide a higher combination rate and less rigid fixation requirements, but the technical requirements are higher. C1-C2 fixation utilizing crossing C2 laminar screws offers unbending fixation yet without the higher technical requirements of C2 standard placement [6].

Providing a stable instrument is one of the possible solutions in practice. But the variable C1 and C2 anatomy can make instrumentation challenging and prone to potentially severe complications [7]. Magerl and Seeman first presented this strategy in 1987 and a C1 lateral mass screw fixation method was portrayed by Harms in 2001. Zarro et al. [8] evaluated the biomechanical stability that unicortical lateral mass and posterior arch screws are viable options for fixation. To perform this, neurosurgeons must be well experienced in the identification and their judgment for the navigation

path should be highly precise, which is a big challenge. For this, neurosurgeons required pre-operative planning. The classification can be done based on part-segmentation to identify the cervical spine from C1-C7. Further, for trans articular screw fixation within C1 and C2, neurosurgeons must investigate each path for all CT (computed tomography) scan slices carefully, so that the screw should not be close to any critical edge of the bone. The objective of the project is to provide neurosurgeons with *3D pre-operative planning of C1-C2 pedicle screw fixation* and *AR/VR (Augmented Reality/Virtual Reality) real-time 3D navigation* during surgeries.

### 1.1 3D Object Representation – Point Cloud

3D object can be expressed as many forms in computer system such as *polygon mesh*, *voxel*, and *point cloud*. Voxel is an abbreviation for volume pixel. Conceptually similar to 2D pixel which the smallest unit used in 2D images, a voxel is the smallest unit of 3D spatial partitioning. Like pixels, voxels do not contain 3D coordinates in space, making it difficult to use screw path planning within a 3D vertebra. 3D meshes are geometric data structures most often composed of a bunch of connected triangles that explicitly describe a surface, which are often used for geospatial reconstruction for video games. This format also does not contain 3D coordinates, so 3D screw path planning is not easy to design. A point cloud is a set of points to represent an object in 3D space. Each point has its Cartesian coordinates (X, Y, Z). Point clouds data can be generated from mesh files using Open3d python module [9] and can be used in a wide range of applications as shown in Fig. 1.

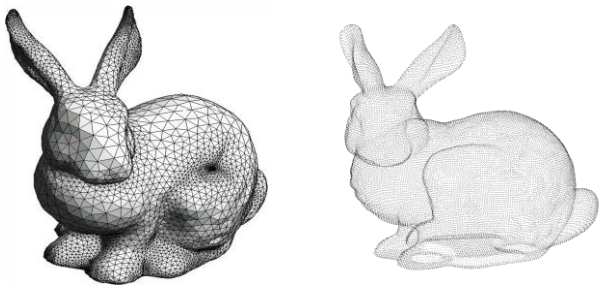

Fig. 1. Rabbit (L) mesh visualization (R) Point cloud

### 1.2 Part Segmentation

*Semantic segmentation* refers to the task of assigning a class label to each pixel in an image. This is a conspicuous difference to the arrangement, where a single label is appointed to the entire picture. Semantic segmentation is the classification of which points in an image belong to which objects while *part segmentation* is to classify which points in an object belong to which sub-objects as shown in Fig. 2. Typically, part segmentation is harder than semantic segmentation. Part segmentation adds a mask forecast based on objective discovery, which can precisely section the edge of the objective, the recognition result is more exact, and can more readily deal with impediment issues between targets [10].

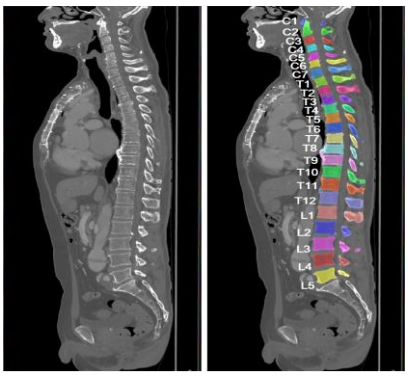


Fig. 2. (a) CT original spine image (b) Segmentation into different vertebrae [39]

### 1.3 PointNet

PointNet is the first to use point clouds as data for training [10], [11]. It solves the two major problems of learning point clouds in neural networks, the disorder, and rotation of point clouds. For a point set containing *N* points, the expression order of each point does not affect the entire point set. In other words, a neural network based on feature learning of point clouds should remain invariant to point clouds with different expression orders. For a point cloud with *N* points, the order of expression has the order of *N* factorial species, so the neural network needs to keep the order of the *N* factorial species unchanged. The author proposed the concept of symmetric function. If the entire neural network is a symmetric function, then it can maintain the invariance of the order of the input point cloud. In the same reference coordinate system, the rotation of the point cloud will cause the inconsistency of the coordinates. Therefore, the designed neural network must also maintain the invariance of any rotations. The three-dimensional STN [12] can learn the pose information of the point cloud itself and learn a rotation matrix that is most conducive to the classification or segmentation of the network.

### 1.4 Unsupervised Labeling of data

The models, which can label the data without any human intervention, are known as unsupervised learning. Interestingly, the benefit of unsupervised segmentation is that the data can be properly segmented without the need for a labeled dataset. Such methods are more applicable to unseen situations, suitable for various classes of medical images. However, it may not be effective when segmenting certain categories of images; therefore, some algorithms need to be introduced to optimize the results.

### 1.5 3D Data Augmentation

*Data augmentation* (DA) is a technique that increases the amount of data by adding modified copies of existing samples and acts as a regularizer that helps reduce overfitting when training machine learning models. Many techniques have been used for 2D DA, such as translation, rotation, mirroring, and resizing. However, 3D DA is much more complicated than the 2D DA. For 3D DA on point clouds, many methods apply the same fixed augmentation techniques may be insufficient for training models because 3D images have different shapes from different viewpoints. Considering the nature of 3D point clouds, where data augmentation involves different spatial domains, the authors consider two kinds of transformations on point cloud samples: transformations in shape direction (including rotation, scaling and their combination) and displacement in point direction (point position jitter), thus improving the effectiveness and robustness of machine learning [13].

### 1.6 Augmented Reality and Virtual Reality

AR is a technology that incorporates digital data into the user's real-world surroundings. It has

become a widely debated subject in our culture, as well as a fertile ground for new medical apps. This proposes a novel method for medical treatment and teaching. AR aids in surgical planning and patient treatment, as well as assisting patients and their families in understanding difficult medical conditions. Due to rising stress in public health systems, there is a strong need for aiding systems, which is one of the reasons for AR and VR rapid growth [14] [15].

### 1.7 Major contributions of this research

(a) Extraction of cervical spine by filtering skull, teeth, lumbar, thoracic vertebrae from 2D CT images.

(b) Reconstruct 3D cervical spine and part-segment spine into C1-C7 cervical vertebrae. The spine segmentation is challenging as the neighboring vertebrae usually share similar morphological appearances, and the dataset is very less.

(c) Due to a smaller number of data, we use an unsupervised method for part-segmentation of C1 and C2.

(d) Part-segmentation of C1 and C2 using deep learning approach to reduce computation time and increase accuracy.

(e) For the pedicle screw path planning, we propose a technique to select critical points based on the centers of the largest/smallest cross-section area in posterior arch, lamina, and lateral mass. Screw navigation path achieved by joining the critical points in each respective side of vertebrae.

(f) The calculated critical points can increase labeling data for deep learning approach to predict the critical points of new patients.

(g) Critical points predicted from deep learning are used for further screw path planning of new patients.

(h) To provide a 3D visualization to neurosurgeons, we have used AR technology that the screw planning path is projected on the patient's real cervical spine to assist neurosurgeons in performing surgery.

## 2. Project goals

The three-year project goals and corresponding designed functions are shown in Fig.3 and will be explained in detail as the following subsections.

### 2.1 1st Year Goal

The goal of the first year is to do extraction of C1 and C2 by filtering skull, teeth, other vertebrae from 2D DICOM images and then reconstructs 3D spine images and part-segment spine into C1-C7 cervical vertebrae and further computes pedicle screw insertion path in C1 and C2. U-Net is employed for extraction of cervical vertebrae from the DICOMM images and PointNet is employed for extraction of C1 and C2. For part-segmentation, we have

employed unsupervised model (k-means clustering) to part-segment C1 and C2 into their anatomical parts. We know that supervised deep learning requires large amounts of labeled data. However, it is challenging for neurosurgeons or technicians to label the large number of the anatomical parts of C1 or C2. Therefore, we designed our model in this way to part-segment the C1-C2 vertebrae using an unsupervised machine learning model. Then, we design a method to find the navigation path where the instrument can be inserted.

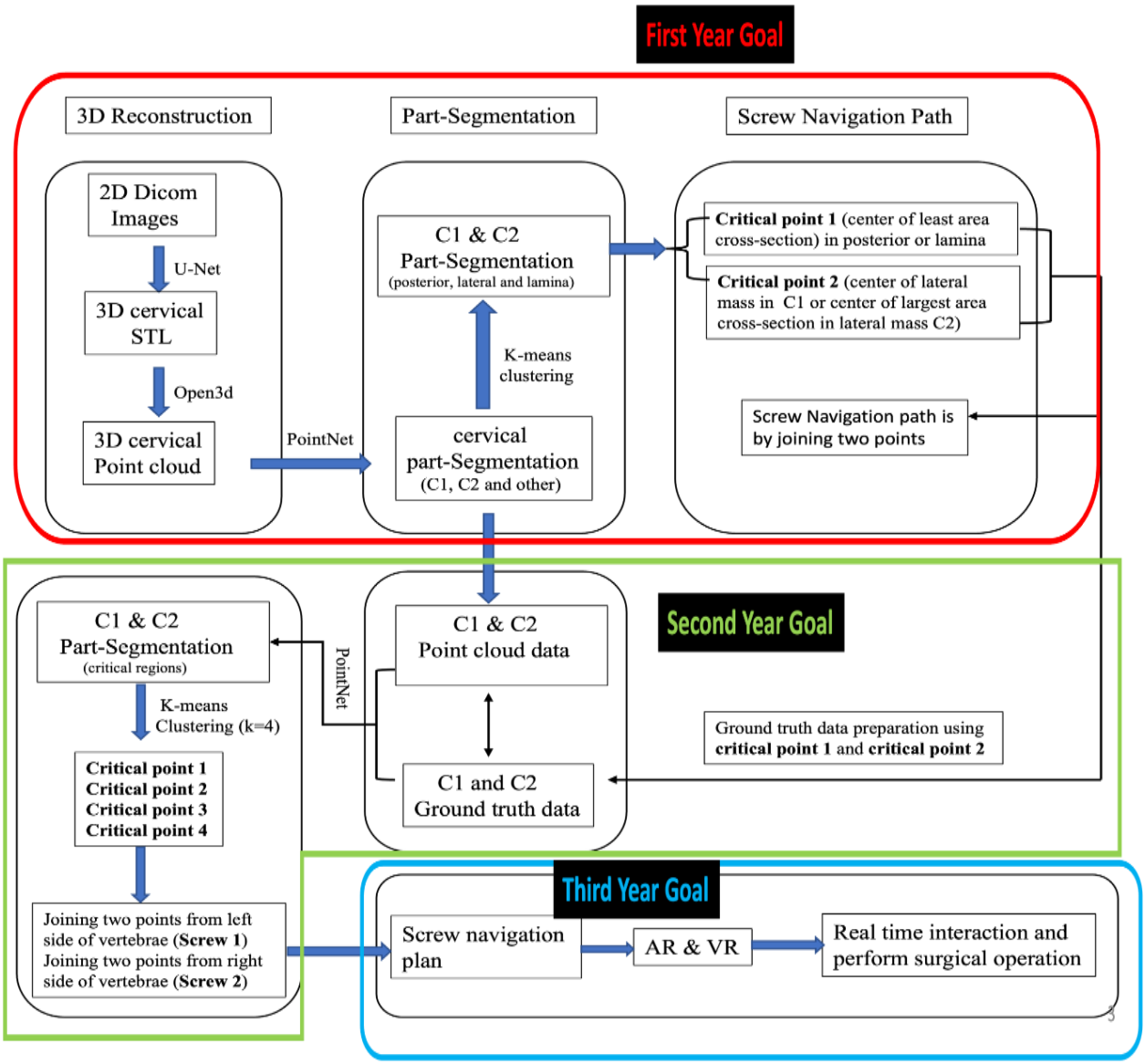


Fig. 3. Three-year project goals and corresponding designed functions

## 2.2 2nd Year Goal

In the second year, the goal is to use the deep learning model to predict critical points and further derive the screw navigation path so that the vertebrae are not broken and firmly fixed. We use the critical points predicted by the unsupervised approach to prepared label data for deep learning model training. PointNet model is employed to do part-segmentation into

critical regions (the posterior arch, lateral mass, and lamina) in C1 and C2 vertebrae and then k-means clustering is used to find the critical points to achieve the screw navigation path. To evaluate the performance of proposed methods, the predicted screw navigation results will be compared with the actual screw navigation results. After analyzing the navigation results by surgeons, screw placement surgery can be performed.

### 2.3 3rd Year Goal

In the third year, our objective is to provide a system that integrate the automatic pedicle screw path planning developed in the first and second years with AR real-time navigation during surgeries. To this end, the screw planning path is projected on the position of the patient's real cervical spine to assist neurosurgeons in performing surgery, so the neurosurgeons can view the 3D spine image overlayed on patient's real spine through the AR helmet even when moving around.

## 3. 1st Year Project: Pedicle Screw Navigation Planning using Unsupervised Method

### 3.1 Background

The cervical spine is a vital organ in the human body that controls numerous physiological functions. It connects the head to the rest of the body and ensures flexibility of the neck and movement of the head. If there is an injury in the cervical area, it will result in tetraplegia/quadriplegia, which means limited or no sensation or movement below the shoulders/neck [16] Causes include motor vehicle accidents (36–48%), violence (5–29%), falls (17–21%), and recreational activities (7-16%) [17]. Due to the advancement of modern medicine, most of these patients can survive; but many will have sequelae of quadriplegia.

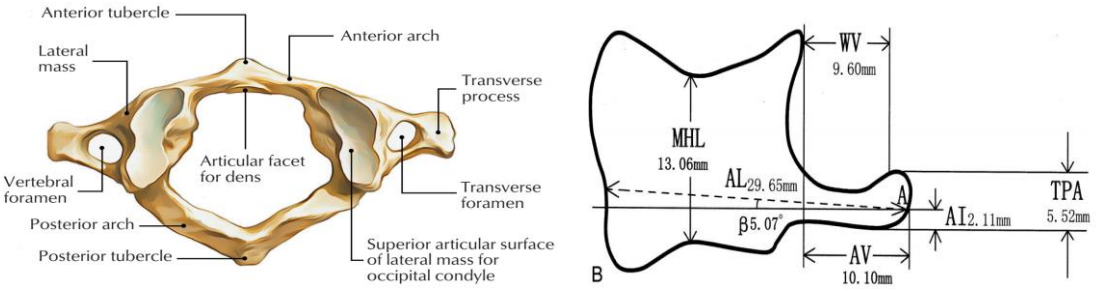


Fig. 4. (a) C1 spine anatomy (b) Measurement required for the screw insertion [8]

According to statistics [18], every year in the world, there will be 10.4 to 83 spinal injuries per million people; 1/3 of them become quadriplegic, with limbs unable to move. Therefore, fixation surgery after cervical spine injury is particularly important. The cervical spine can be classified into C1 to C7 from top to bottom. C1 and C2 are very special vertebrae because they have some distinguishing features compared to the rest of the cervical spine. The atlanto-

occipital joint is formed when C1 connects to the superior occipital bone to support the skull base. The odontoid process on C2 points up from its vertebral body and fits into the ring-shaped atlas above it [1]. Injury to the cervical spine necessitates surgery to repair the cervical spine. Cervical spine fixation has necessitated a plan for the operation's path, which is time-consuming, labor-intensive, and inaccurate [19]. The procedure is performed through a posterior approach with the patient placed in the prone position.

Magerl first described the use of trans articular screws [20]. The C1-C2 joint can be fixed in this way, which is simple and inexpensive. However, the screw insertion requires the use of fluoroscopy. In addition, the C2 pars must be large enough to accommodate a 3.5 mm screw. In the past, many studies on cervical spine fixation have been achieved. For example, by measuring a large amount of data between the posterior arch and lateral mass in C1 for surgery [8], [21]. The spine anatomy of the C1 cervical spine is shown in Fig. 4(a). In Fig. 4(b), the required measurement for the screw insertion. However, all these methods necessitate a significant amount of time and manpower to complete preoperative planning. Fixed surgery is a surgery that requires very high accuracy, and manpower will inevitably cause errors. A set of automatic planning and fixation of the cervical spine path system is required to avoid human errors. Therefore, our unsupervised approach can automatically plan the best path and assist the doctor to make fine adjustments. To achieve this, we need image representations with 3D structures and coordinates. In our system, we automatically reconstruct 2D CT images into a 3D point cloud object. To further segment C1 and C2, a two-stage deep learning neural network is used on the reconstructed 3D cervical spine. Due to a smaller number of data, we use unsupervised method to do part-segment the C1 and C2 vertebrae. After segmentation, we propose an unsupervised approach for automatic path planning, based on the geometry shape of patients. We directly process the raw data of the point cloud of C1 and C2 and use unsupervised method to identify the anatomy of the vertebrae. Then, based on the medical foundation provided by clinical guidelines [8], [20], find the critical points of the surgical path planning, to achieve the purpose of automatic planning.

### 3.2 Related work

Regarding the identification of cervical spine injuries, there is a study [22] for children aged 2-18. After scanning them with CT images, the C1 and C2 parts were manually measured on both sides of the lateral mass and the distance to the dens. Studies have shown that the distance of a healthy cervical spine should be 1.7~2.7mm and the distance of an injured cervical spine should be 2.5~4.1mm. There is a significant difference between the two, which can be used as a basis for distinguishing whether the cervical spine is injured. Image segmentation is performed accurately by judging the category of each pixel in the image.

Different pixel values may represent different parts, such as cervical vertebrae, teeth, etc [23]. In the classification of 2D images, ResNet [24] has surpassed humans in the performance of deep learning for classification tasks, but the accuracy of target detection tasks and segmentation tasks has been low. In response to the needs of semantic segmentation, Fully Convolutional Networks (FCN) first proposed by Jonathan Long [25] and many subsequent frameworks have somewhat referenced the idea of FCN. However, the accuracy of FCN is low, and it is not as widely used as U-NET [26] which is one of most important semantic segmentation by using convolutional neural network and perform very high accuracy for biomedical image segmentation. In this study [27], authors have focused on image processing and computer vision by having high precision dynamic registration for image navigation. For image registration, the matching methods based on feature and grey have been studied. Literature [28] has introduced 3D technology based on 3D reconstruction and 3D printing for clinical treatment especially in surgical planning, and image navigation technology, which can make surgical procedures more accurate. The model is more helpful than the CT/MRI images in the surgical discussion, preoperative planning, clinical teaching.

In this proposal, we are using unsupervised approach to do part-segmentation of C1 and C2 vertebrae anatomy. Due to smaller number of data, supervised approach needs huge amount of data to do classification and segmentation task. Accuracy of classification and segmentation task is directly proportional to number of training data with ground truth data. Ground truth data preparation for point cloud data required a lot of computation and time. But in this proposed approach, the segmentation task can perform with one data.

The combination of 3D technology and electromagnetic image guidance system improves surgical efficiency and the quality of clinical teaching. In [29] study, authors have proposed image guidance and robotics systems during the surgery process. The objective of this is to reduce the incidence of malposition screws, less is known about their impact on clinical outcomes. While using these technologies to guiding thoracolumbar pedicle screw placement, but also in cases of cervical and pelvic instrumentation as well as spinal tumor resection. This results in improving surgical accuracy and clinical outcomes against concerns over cost and workflow. In the research article [30] the authors have discussed stabilizing by a different technique. The most common technique is the lateral mass screws (LMS), the freehand technique. The objective of this study is to evaluate the 3D navigation system and the freehand technique for cervical spine LMS placement in terms of complications. The results show that the use of CT-based navigation in LMS insertion decreased the rate of screw malposition's. In a study [31] authors proposed a 3D-CT reconstructive rapid prototyping drill template for cervical pedicle screw placement. The ideal screw channels were chosen by analyzing the

cross-sections of the reconstructed 3D images, later optimal screw channels have designed. The authors have also provided the comparison based on Entry point and exit data points. However, the study has not considered the point cloud dataset and, not following the minimal invasive rule, there is no test cases have been evaluated. In this work [32] authors proposed a 3D printed navigation template with two guide tubes and the guiding group was treated with pedicle screw with the assistance of virtual reality (VR) software designed. This work is mainly focused on type II odontoid fractures. The 3D model of the cervical vertebrae was virtually generated. Then the insertion channel of the cylinder was carefully analyzed and adjusted in the sagittal, coronal, and axials views. The insertion guide tube was then reconstructed according to the preset axial trajectories and accurately configured with the template to form the complete navigation 3D template. However, in this work they relied only on software for template design. In this work [33], authors proposed a novel technique of atlantoaxial stabilization using individual fixation of the C1 lateral mass and the C2 pedicle with minipolyaxial screws and rods is described. After posterior exposure of the C1–C2 complex, the 3.5-mm polyaxial screws are inserted in the lateral masses of C1. Two polyaxial screws are then inserted into the pars interarticularis of C2. Drilling is guided by anatomic landmarks and fluoroscopy. If necessary, reduction of C1 onto C2 can be accomplished by manipulation of the implants, followed by fixation to the 3-mm rod. However, in this work for each patient they need to perform manually screw placement. This study [34], was performed to determine the optimal entry points and trajectories for cervical pedicle screw insertion into C3- C7. A surgical simulation program was used to construct three-dimensional spine models from cervical spine axial CT images. Axial, sagittal, and coronal plane data were simultaneously processed to determine the ideal pedicle trajectory. However, this work has not considered the C1-2 vertebrae. There is not any robust method for C1-2 pedicle screw fixation. All these methods of pedicle screw path planning often require manual operation to obtain single vertebrae in spine images. Most of these methods are applied according to the statistical regularity for path planning, which cannot achieve fully automatic processing and will cause problem when addressing the specificity of different vertebrae.

In this proposal, an automatic pedicle screw path planning method is proposed based on point cloud data to solve the problems related to the complicated procedures and poor universality of the path planning method in current pedicle surgeries.

### 3.3 Data and Material

Clinical data and DICOM images were collected at Chang Gung Hospital for analysis. The patient's CT scan with destabilization in CS especially in C1 and C2 vertebrae has been captured. Currently, for 50 patients we have the CT scan images. Each patient has around

700~1100 DICOM images.

### 3.4 Data Cleaning

CT images have some parts that belong to the skull, teeth, and jaw, which are not needed in our analysis. Thus, we need to do data cleaning over CT images to remove the skull, teeth , and jaw as shown in the right part of Fig. 5. The doctor has provided us CT DICOM images of 50 patients. To better convert 2D CT/MRI images into 3D format, we use U-Net [26] to filter skull or teeth parts from 2D CT images to extract the cervical spine. The part of the cervical spine is identified through the automatic grouping method.

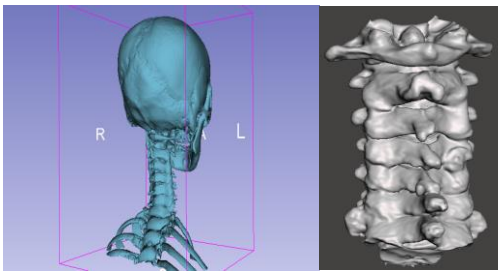


Fig. 5. (L) The raw image from CT/MRI (R) Cervical Spine

Due to the characteristics of the CT image, there are other soft tissue components and bones such as teeth in addition to the cervical spine. In order to effectively distinguish the cervical spine from other bones, we find the dividing line between the cervical spine and the teeth, and thanks to the special and obvious ring structure of the cervical spine, we identify the continuity of the pixel values in the CT image to find out the Center, and filter the parts that do not belong to the cervical spine one by one through the pixel by pixel method, and finally mark the cervical spine as 1 and the rest as 0. After U-Net training, the CT images obtained from the prediction results are stacked to obtain a complete 3D cervical spine in STL format and then convert to point cloud format using open3d python module Fig. 6.

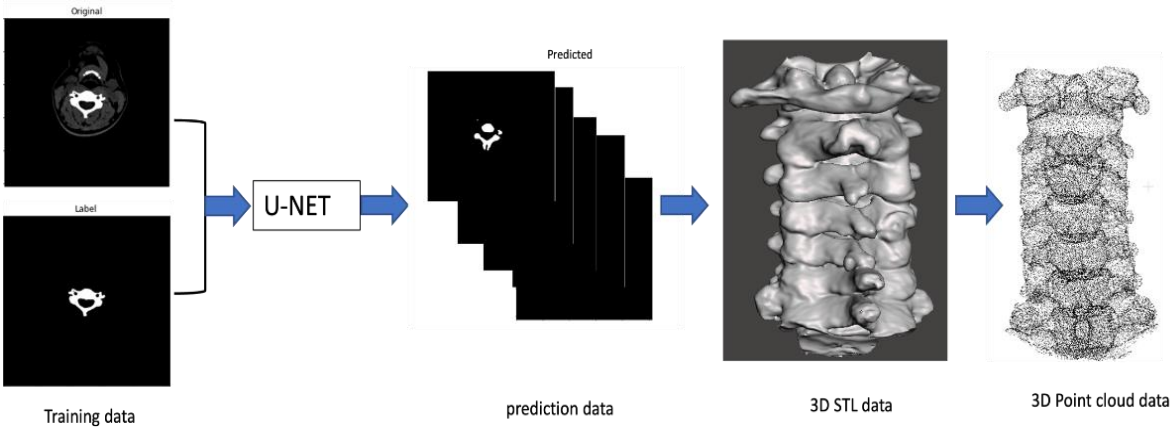


Fig. 6. Dicomm images to 3D point cloud data

### 3.5 Part-segmentation of Cervical Spine

In this stage, we input the 3D point cloud of cervical spine data into the PointNet [12] for

part-segmentation into C1, C2 and C3-C7 as shown in Fig. 7. For automatic screw path planning in C1 and C2, we further need to part-segment of C1 and C2.

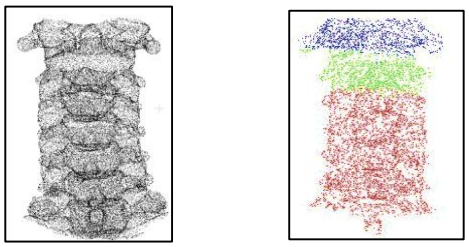

(a) (b)

Fig. 7. Part segmentation and classification (a) 3D point cloud CS, (b) part-segmentation into C1(blue), C2 (green), C3-C7 (red)

### 3.6 Part-segmentation of C1 and C2 using unsupervised method:

In this stage, we segment C1 and C2 from the cervical spine and again we need to part-segment the C1 and C2 into posterior arch, lateral mass, and lamina as shown in Fig. 8. We employed K-means clustering (unsupervised method) to perform part-segmentation on C1 and C2 vertebrae. Unlike, in training of Deep learning method (supervised approach), need huge amount of data to perform classification, segmentation or object detection task. Due to a smaller number of C1 and C2 data, unsupervised method can perform segmentation task on one data with more efficiently compared to supervised method.

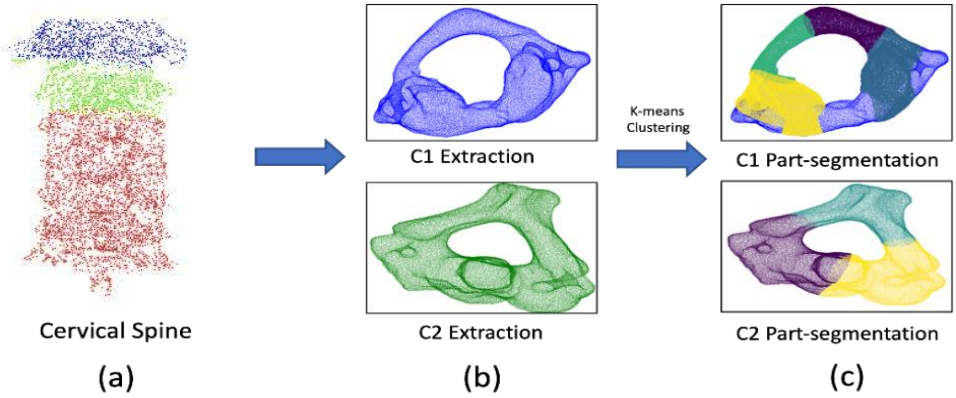


Fig. 8. (a) segmentation and part-segmentation of CS, (b) segmentation/extraction, (c) C1 part-segment into posterior arch (green, purple) and lateral mass (yellow, deep blue) and C2 part-segment into lamina and lateral mass (purple, yellow)

#### 3.6.1 Pedicle Screw Navigation Design in C1 and C2:

The idea to design the screw navigation path in C1 and C2 is to place the screw in vertebrae without breaching and damaging artery or sensitive tissues. For that find the smallest cross-section in posterior arch of C1 and lamina of C2 and largest cross-section in lateral mass in C1 and C2. For screw navigation, we need to find the center of smallest ross-section and largest cross-section as

*entry* and *exit* point, respectively. By joining the two points, also called *critical* points, we will achieve the screw navigation path without breaching the vertebrae in both C1 and C2.

**Find the smallest cross-section in posterior arch:**

First, we need to extract the posterior arch Fig. 9. from the part segmented C1. After that the surface data points are collected from the posterior arch. We employed the 3rd degree polynomial curve to fit the data points. Once we have the curve on surface, we divided the posterior arch into several cross-sections by drawing normal lines to the curve. All the data points nearest to the normal line is treated as one cross-section. There are number of cross-sections in the posterior arch, and we need to calculate the center and area of each cross-sections Fig. 10. The cross-section with the least area will be the critical part of posterior arch and the screw must pass through the center (critical point 1) of the least area cross-section to avoid the breaches of the vertebrae.

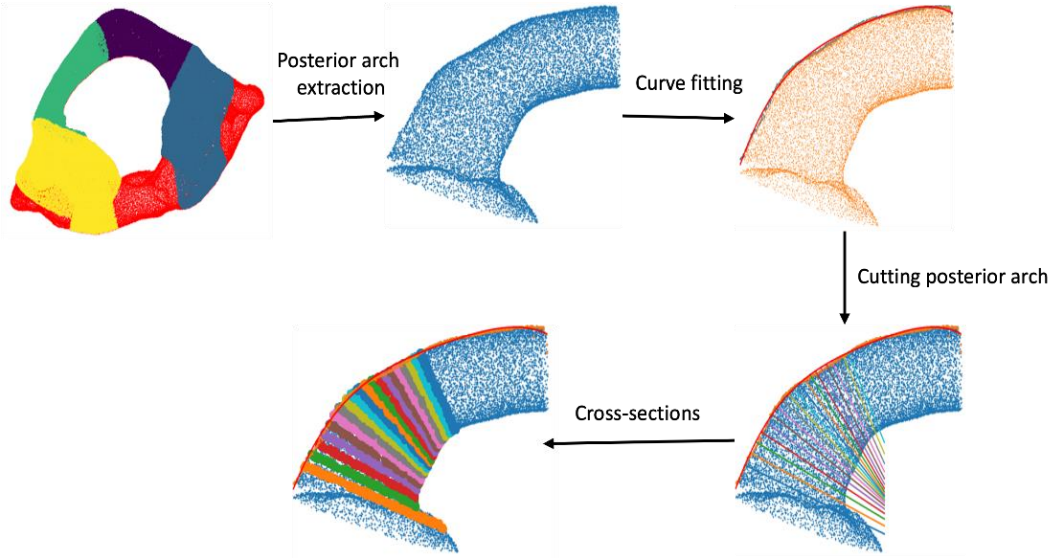


Fig. 9. cross-sections in posterior arch

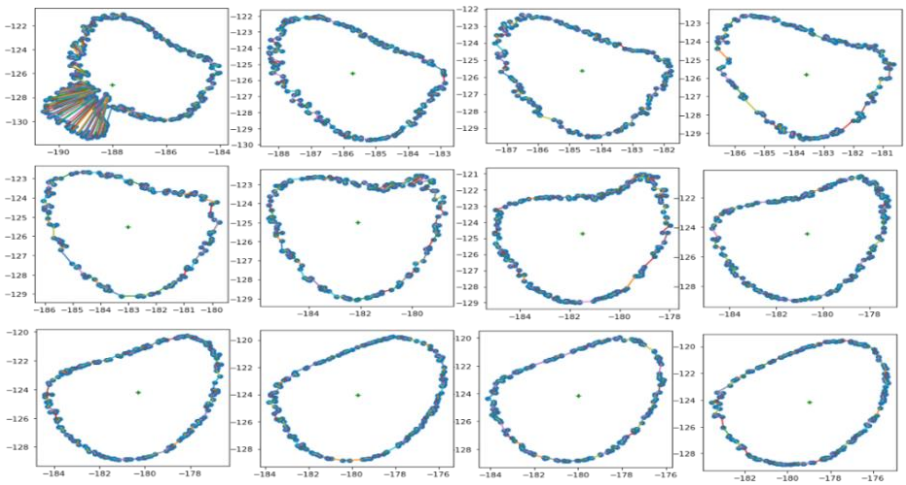

Fig. 10. cross-sections from the posterior arch

**Area of irregular polygon:** To find the area of irregular polygon, we need the position of vertices;

its equation is shown as follows,

$$W = \frac{1}{2}\sum_{i=0}^{n-1} \det(v_i, v_{i+1}) \qquad (1)$$

where, $W$ = Area of polygon, $n$ = number of triangles, $v$ = vertices of triangle. This above equation helps to find the area of each polygon.

**Find the center of mass in lateral mass:** First we extracted the lateral mass from the part segmented C1 vertebrae. After that, we employed k-means clustering algorithm to find the center of mass in lateral mass Fig. 11.

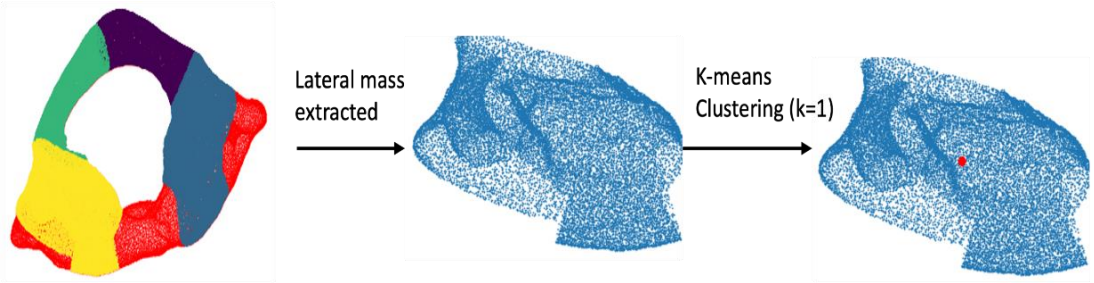


Fig. 11. Lateral mass of posterior arch

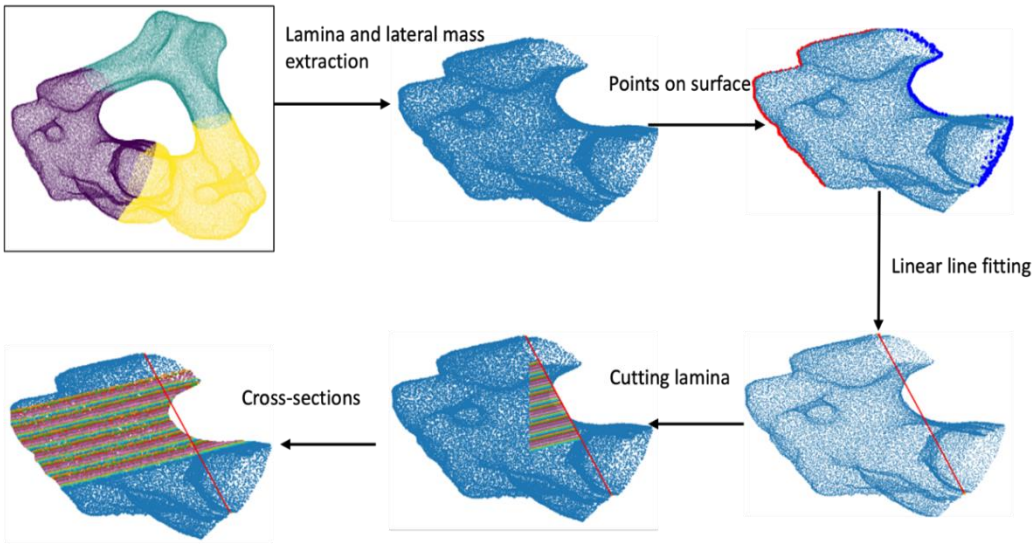


Fig. 12. Cross-sections in lamina

**Find the smallest area cross-section in lamina:**

Fig. 12 shows the process of finding the smallest area cross-section. First, we need to extract the lamina and lateral mass. from the part segmented C2. After that the surface data points are collected from the lamina and lateral mass. We employed the linear equation to fit the first and last points. Once we have the line on surface, we divided the lamina into several cross-sections by drawing normal lines to the curve. All the data points nearest to the normal line is treated as one cross-

section as shown in Fig. 13. There are number of cross-sections in the lamina, and we need to calculate the center and area of each cross-sections. The cross-section with the least area will be the critical part of lamina and the screw must pass through the center (critical point 1) of the least area cross-section to avoid the breaches of the vertebrae.

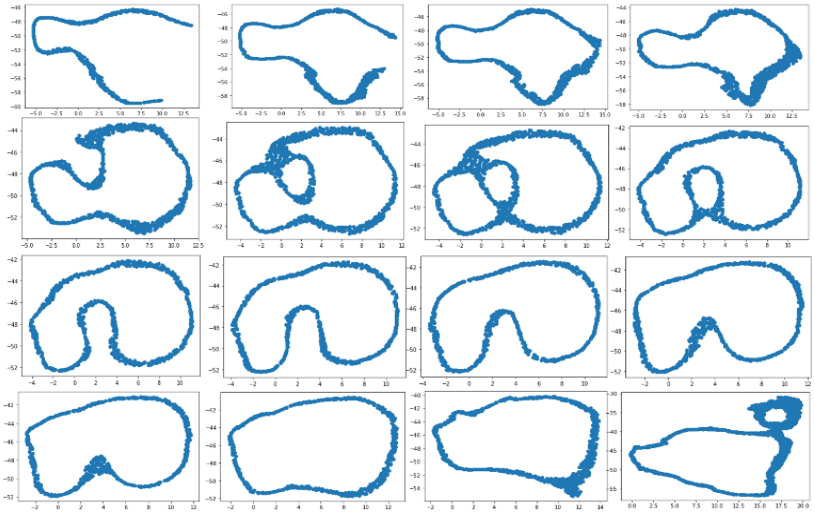

Fig. 13. cross-sections from the lamina

**Find the largest area cross-section in lateral mass:**

We need to extract the lamina and lateral mass from the part segmented C2 as shown in Fig. 14. After that the surface data points are collected from the lamina and lateral mass. We employed the linear equation to fit the first and last points. Once we have the line on surface, we divided the lamina into several cross-sections by drawing normal lines to the curve. All the data points nearest to the normal line is treated as one cross-section as shown in Fig. 15.

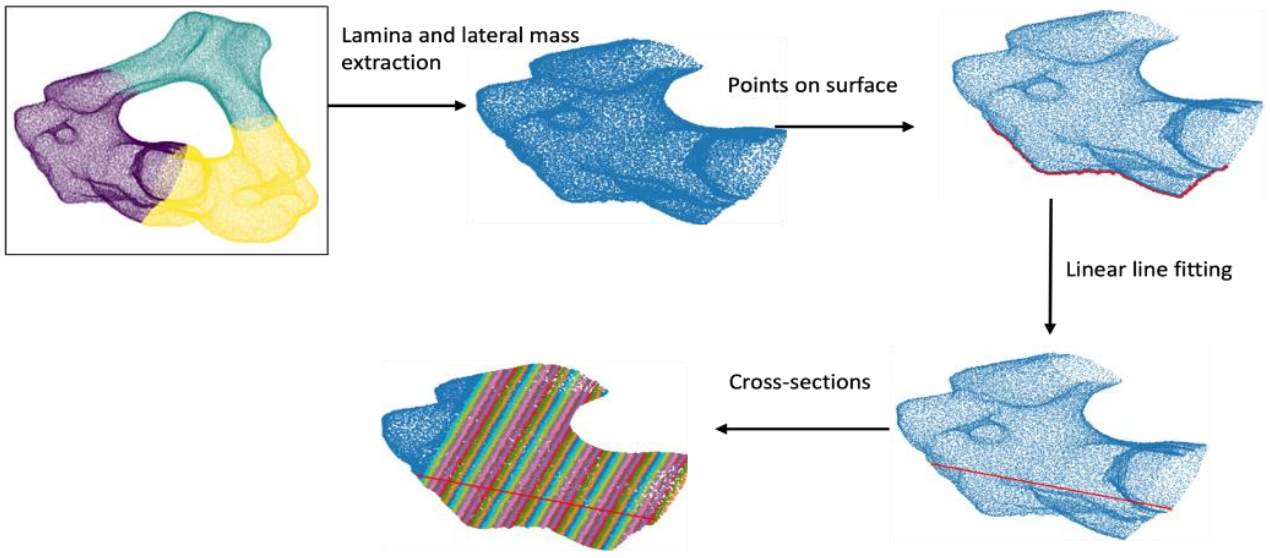


Fig. 14. Cross-section in lateral mass (C2)

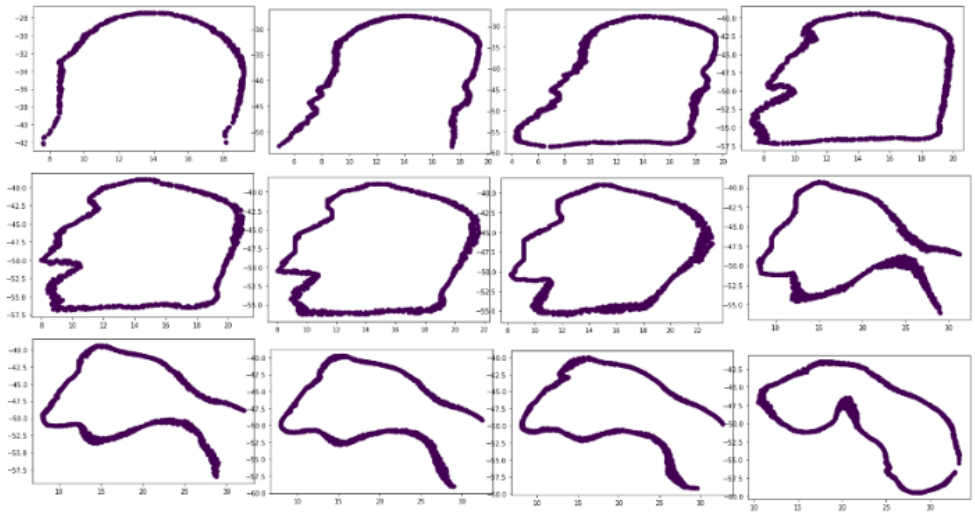

Fig. 15. cross-sections from the posterior arch

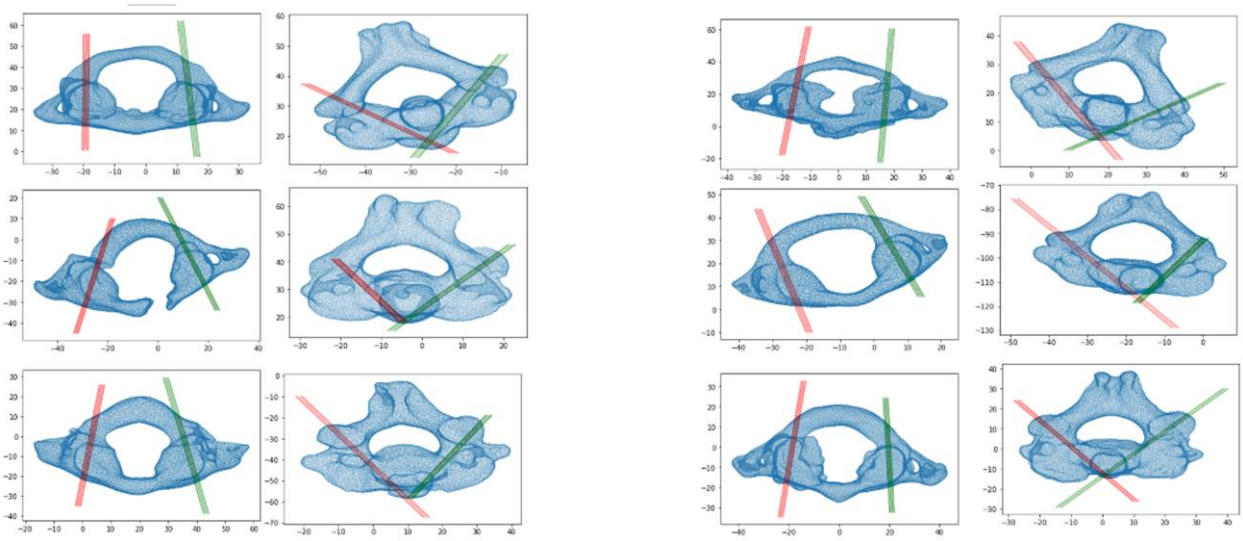

(a) red line = screw 1, green line = screw 2

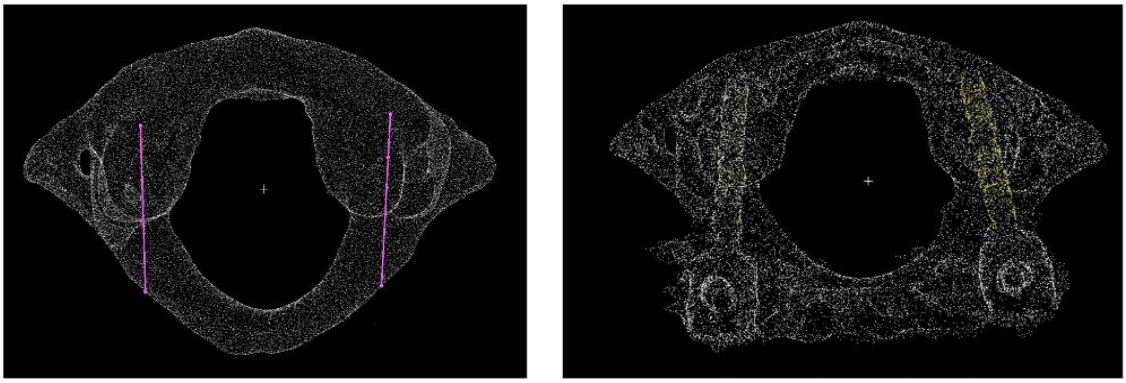


(b) Actual vs Proposed screw navigation

Fig. 16. The Preliminary Results of the First Year project

### 3.7 Preliminary Results:

In this section, we show the preliminary results of the screw navigation paths as shown in Fig. 16. The screw navigation paths in C1 by joining the critical point 1 in posterior arch and critical point 2 in lateral mass and in C2 by joining the critical point 1 in lamina and critical point 2 in lateral mass. The critical point 1 and 2 also are called entry and exit point, respectively. Fig. 16 (a) shows the pedicle screw navigation of this proposed approach and Fig. 16 (b) give one pair of our design and the actual screw placement of patient. Table 1 gives the differences between the predicted/actual entry/exit points of patients who recovered well during hospitalization. The preliminary results were approved by the clinical neurosurgeons. In the future, we will further evaluate our results by using the clinic grading system which was created to objectively describe this disruption by the percentage breaches beyond the cortical edge [35]. Also, we will compare more patients who recovered well during hospitalization.

Table 1. Differences between the predicted/actual entry/exit points (Unit: mm)

| Patient ID | Right Screw | | Left Screw | |
|---|---|---|---|---|
| | Entry_diff | End_diff | Entry_diff | End_diff |
| 1 | 0.92 | 2.26 | 0.86 | 2.53 |
| 2 | 1.12 | 2.31 | 0.75 | 2.94 |
| 3 | 1.22 | 2.42 | 1.24 | 2.37 |
| 4 | 0.84 | 2.13 | 1.35 | 2.62 |
| 5 | 0.79 | 2.14 | 0.72 | 2.43 |
| Avg | 0.98 | 2.25 | 0.98 | 2.58 |

## 4. 2nd Year Project: Pedicle Screw Navigation Planning using Supervised Method

### 4.1 Related Work

In the second year of the project, we have surveyed many research papers related to the pedicle screw fixation using AI. In this work [36], they proposed an automatic path planning method of pedicle screw placement based on preoperative CT scans, the spine of the patient can be segmented, and each individual vertebra is classified by using a trained deep learning network model. Additionally, a local coordinate system in every single vertebra is established according to its anatomical characteristics. Second, after analyzing the images to recognize the feature points, the pedicle region and route of screw placement are identified, which renders completion of the surgical path planning automatic. But this work was mainly focused on vertebrae's which are structurally similar. A variety of methods for automatic spine screw planning have been reported [37]–[40]. In [37], the computer-assisted preoperative planning tool can achieve acceptable pedicle screw placement in 96.6% of cases. With the application of 3D modeling of the vertebral body and pedicles, Wi et al. [38] have also developed a

preoperative planning system that enables real-time interaction with surgeons, which can help guide less-experienced surgeons in pedicle screw fixation. Authors reported the overall accuracy of screw placement to be 96.4%. However, there have been few studies on automatic planning of screw trajectories with optimal BMD (bone mineral density) and (pull-out force) POF, which will help prevent osteoporosis-related complications. Caprara et al. [39] employed a 3D preoperative planning system to find the optimized trajectories by maximizing the CT-derived bone mechanical properties, and the optimized trajectories had a 26% increase in simulated POF in comparison with AO standard trajectories. Accurate screw placement is of paramount importance to avoid injury to the surrounding neurologic and vascular structures. As such, complications associated with pedicle screw placement are not uncommon and likely under-reported given their widespread use [38]–[40]. Hence, robotics may help reduce pedicle violation, improve accuracy, and prevent associated complications through aids in registration, depth perception, and visual and tactile temporal synchrony [38]**.** To improve pedicle screw positioning, several techniques have been developed, including navigation technologies, such as computed tomography (CT)-guided or robot-assisted technologies. Nolte et al [41] first described computer-assisted image guidance systems in 1995 as a CT-based navigation system. Subsequently, intraoperative CT, such as O-arm and 3D C-arms, were also used in spine surgery for navigation assistance. O-arm [42] navigation provides intraoperative 3D fluoroscopic imaging with an image quality like that of CT, and reduces the time needed for computer-assisted surgery. Wolf et al [43] first reported a robotic guidance system used in spinal surgery in 2004, and robot technology has developed rapidly in recent years, which could decrease the risk of misplaced screws and the associated complications. However, [44]–[46] limited studies have reported the application of robotic-assisted navigation using O-arm or 3D C-arm navigation in scoliosis surgery. In 2019, research [47] first reported an initial intraoperative experience with robotic assisted pedicle screw placement with Stealth navigation (Medtronic Navigation, Louisville, CO, USA) in pediatric spine deformity. They reported that the accuracy rate of the 314 screws placed in the study was 98.7%, and there were no clinically relevant screw-related complications.

### 4.2 Ground Truth Data Preparation

In the second year of the project, we are going to used AI model to predict the pedicle screw navigation path in an automatic way. To used AI model, larger number of training data required with the ground truth data. We already determined the critical points for screw navigation in unsupervised approach. Ground truth data are generated using the critical points as shown in Fig. 17.

### 4.3 Part-Segmentation of C1 and C2 using PointNet architecture

In this stage, we employed PointNet model [12] to perform part-segmentation on C1 and C2 vertebrae. The model is composed of two parts. The main part is segmentation network. The second part is classification network. Due to a smaller number of C1 and C2 data, data augmentation methods like rotation, scaling, resize, and mirror operations are performed on original data to generate more training data. This dataset comes from 50 patients from Chang Gung Memorial Hospital. The total number of training data after data augmentation are 6270 for each C1 and C2 vertebrae. Tensorflow framework is chosen to implement the network model and the whole model are trained on 8 GB NVIDIA GTX2080Ti GPUs. The learning rate was set to 0.001. The training results were obtained after 4-5 hours of 100 epochs with batch size 16.

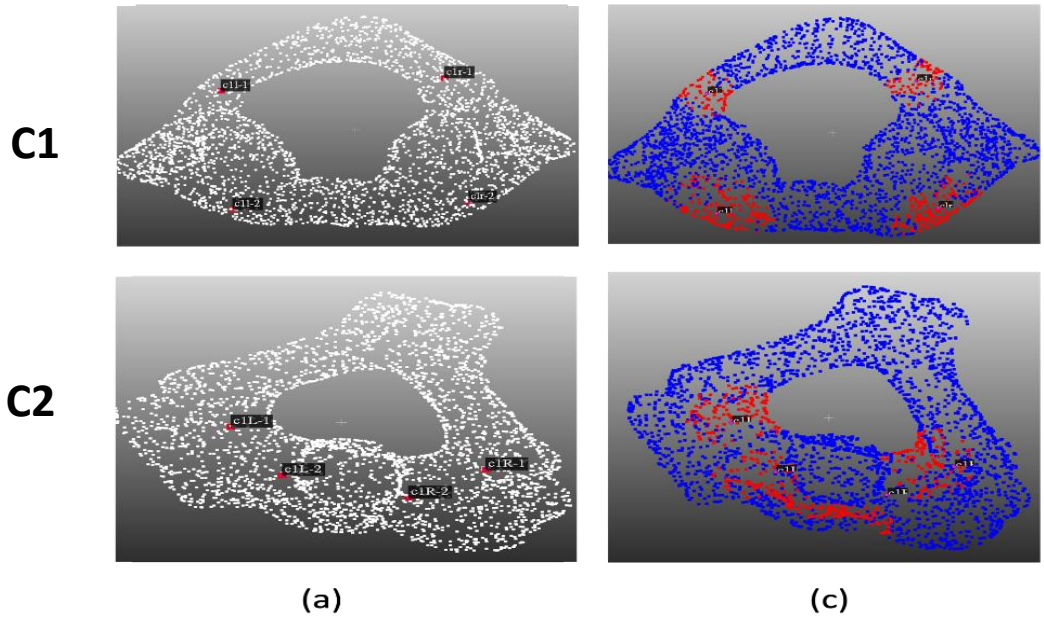


Fig. 17 (a) critical points, (b) ground truth data

### 4.4 Pedicle Screw Navigation Results:

After obtaining the part-segmentation results from PointNet architecture, k-means clustering is used to divide the critical regions into four sub-group. The center of each sub-group are the critical points for screw navigation path Fig. 18.

### 4.5 Preliminary Results

We expect to achieve the screw navigation paths in C1 and C2 by joining the critical points achieved from the sub-group from the part-segmentation of C1 and C2 as shown in Fig. 19. The screw navigation paths of our design will be compared with real data from the neurosurgeons after the operations. Based on the results, we can further improve our design.

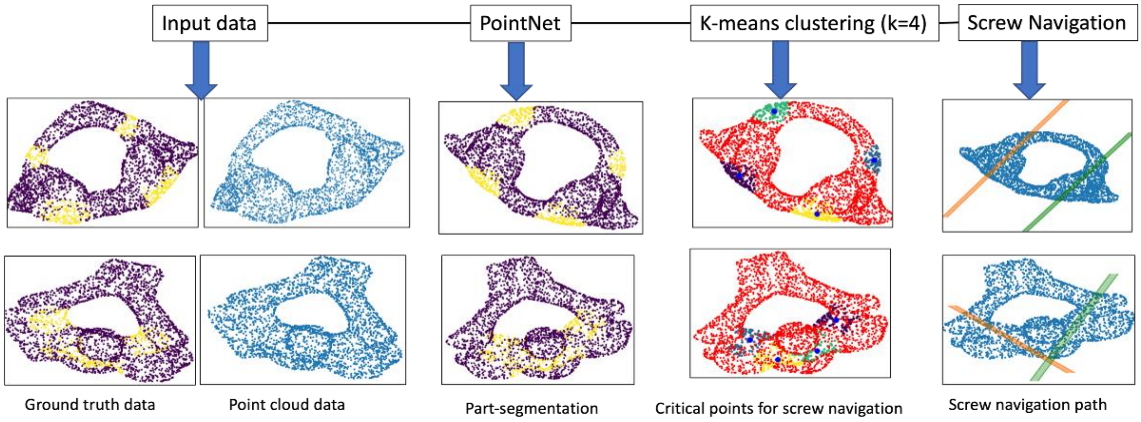


Fig. 18. Screw navigation results

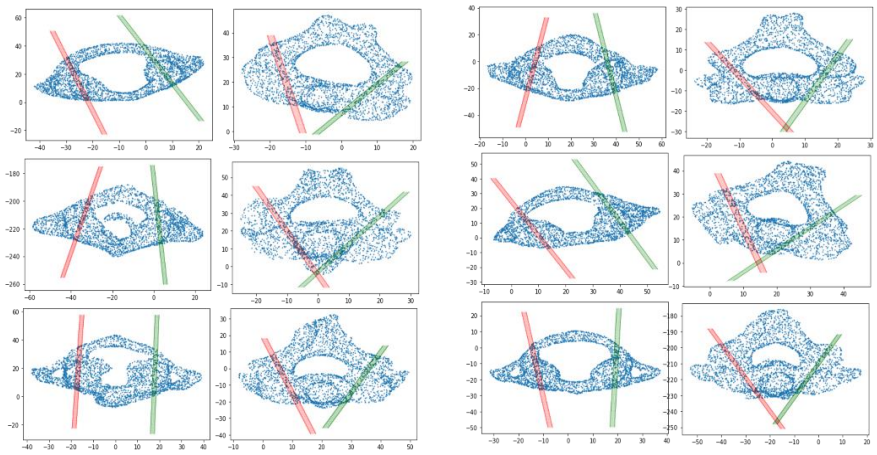

Fig. 19. red line = screw 1, green line = screw 2

## 5. 3rd Year Project: AR Real-Time Screw Navigation

### 5.1 Related Work

Augmented reality (AR), virtual reality (VR) and mixed reality (MR) are new technologies that are beginning to be used in spine surgery [48]. In the third year of the project, we have surveyed many research paper-based AR and VR technologies that support 3D vision and robotic surgery. Many studies have supported the potential advantages of AR- and VR-assisted surgery, including surgical efficacy, target accuracy, safety, and possibilities for surgical training [49]–[50]. However, much of these data regarding these uses and metrics were gathered from studies using animal models, spine phantoms, and/or cadavers with the omission of their full potential for clinical translation on living people.

In this study [51], the authors have provided a historical overview of the evolution of Virtual Reality (VR) and Augmented Reality (AR) technologies, examine their current applications, and evaluate their potential applications in neurosurgery. From trephination to image-guided navigation, neurosurgery has made significant technological advancements in recent decades. VR

and AR are two of the most recent technologies to enter neurosurgery practice and resident education. By allowing neurosurgeons to learn and practice operations in a zero-risk setting, these technologies can help reduce patient risk and surgical mistakes. These technological advancements are unlimited, allowing for efficient and successful real-time navigation in the operating room. Reference [52], authors have discussed the neuro navigation, which functions as a point-to-point navigation system, has become vital in brain surgery. Because the positioning information is shown on a PC monitor, surgeons must rotate the magnetic resonance imaging/computed tomography images to fit the surgery field. They also must switch their attention between the surgical field and the computer monitor regularly. Thus, they proposed an AR-based navigation system to track the surgical area of operation room with expensive VICON system.

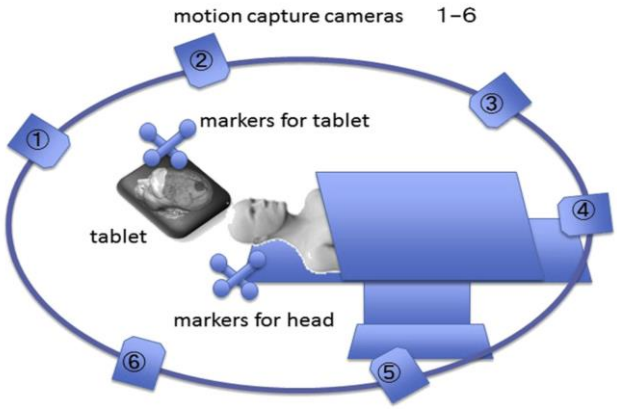


Fig. 20. 6 VICON motion capture cameras are placed on the ceiling of the operation room. Reflective balls are attached to the tablet personal computer and skull clamp [52]

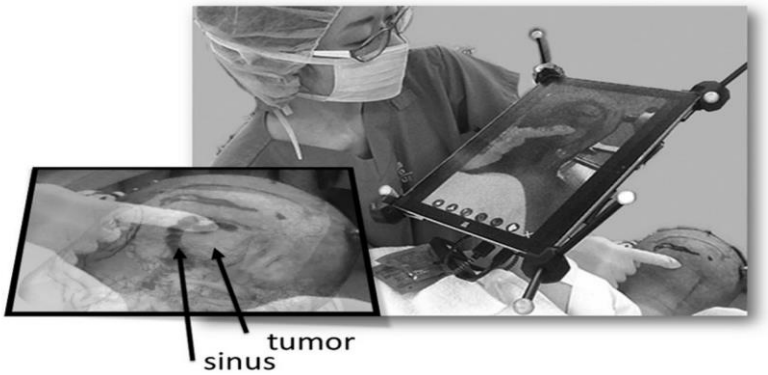


Fig. 21. The surgeon holds the tablet personal computer and views the patient's head through the back-facing camera. Virtual 3D images are overlaid on the video image [52].

In Fig. 20, a tablet is utilized for visualization by its back camera to capture patient's head, which is secured to the operating table. It overlays MRI/CT 3D images of intracranial structures such as brain tumors and blood arteries, directly on real surgical area, allowing the surgeon to naturally merge the two realities. The problem with the proposed system is that it uses the VICON system, which is expensive, complicated and difficult to operate, and it is difficult to promote to general

medical institutions. In Fig. 21, the virtual head's 3D rendered picture is then formed, exactly as it appears on the tablet camera. The resultant head picture is superimposed on the camera picture. The camera picture and the virtual head fit together since the MRI/CT is already in the same location as the actual head.

In study [53] authors investigate the pedicle cannulation that could be done safely and accurately utilizing an augmented reality surgical navigation (ARSN) system with automated instrument tracking that provided feedback on instrument location for deep anatomy. When compared to open surgery, minimally invasive spine surgery (MISS) has the advantage of lowering surgical exposure, resulting in shorter hospital stays, less blood loss, and reduced infection rates, but it has the disadvantage of restricting visual feedback to the surgeon on deep anatomy. The authors recommended using a hybrid operating room (OR) with a robotic C-arm with built-in optical cameras for augmented reality instrument navigation. ARSN with instrument tracking for MISS navigation is feasible, accurate, and radiation-free.

Reference [54] CT images were obtained from a vertebral model consisting of L1-L3 sawed-off vertebrae in opaque silicone. Preoperative planning is performed with virtual trajectories of appropriate angles and depths to achieve ideal pedicle implantation. Planning data was integrated into the Microsoft HoloLens using the Novarad OpenSight application, allowing users to view virtual trajectory guides and CT images superimposed on the 2/3D model as shown in Fig. 22.

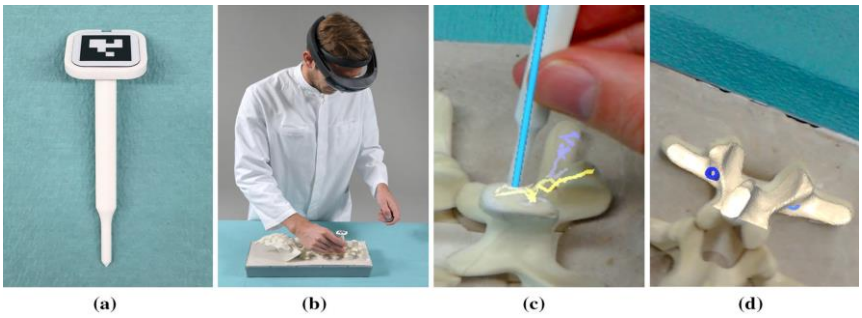


Fig. 22. (a) Pointing device. (b) A surgeon wearing the HoloLens uses the pointing device in the experimental setup. (c) Augmented view of the surgeon during surface sampling. (d) Overlay of vertebra L1 after registration (insertion points are denoted in blue [54]

The OpenSight application downloaded to the HoloLens is used to integrate CT data with AR. In short, the software is the rebundling of CT DICOM images into a proprietary file format, allowing the full integration of the images into a complete single 3D volume. This complete volume rendering is then projected via the HoloLens system, allowing users to visualize the CT reconstructed 3D image. The reconstructed image can be moved in 3D space and can be automatically registered to the object of interest by using an algorithm to align the virtual surface area with the real surface area. This object can then be fixed in 3D space, allowing users to view it even while walking around or in a fixed location.

### 5.2 AR Pedicle screw navigation

We will develop a system that integrate the automatic pedicle screw planning path developed in the first and second years with AR real-time navigation during surgery by using HoloLens and OpenSight in the next third year. The system, as shown in Fig. 23, processes from the input of the patient's cervical spine 2D CT DICOM images, extract cervical spine from original 2D CT images by U-Net, convert 2D CT to 3D point cloud, part-segment cervical spine into C1, C2 and others by PointNet, further part-segment C1 and C2 into posterior arch, lateral mass, and lamina by k-means, and finally produce the preoperative screw planning by supervised learning method, and perform AR navigation during surgical operation. In addition to registration, we also need to address real-time tracking whenever neurosurgeon move his head during operations. For this we need to improve the *epipolar geometry* [55] so that surgeons can visualize the spine at any angle to ensure the safe of pedicle screw placement. The screw planning paths of C1 and C2 are projected to the position of the patient's real cervical spine to assist neurosurgeons to perform surgery, where the patient's cervical spine is fixed in operation bed, so neurosurgeons can view the 3D cervical spine image through the AR helmet even when moving around.

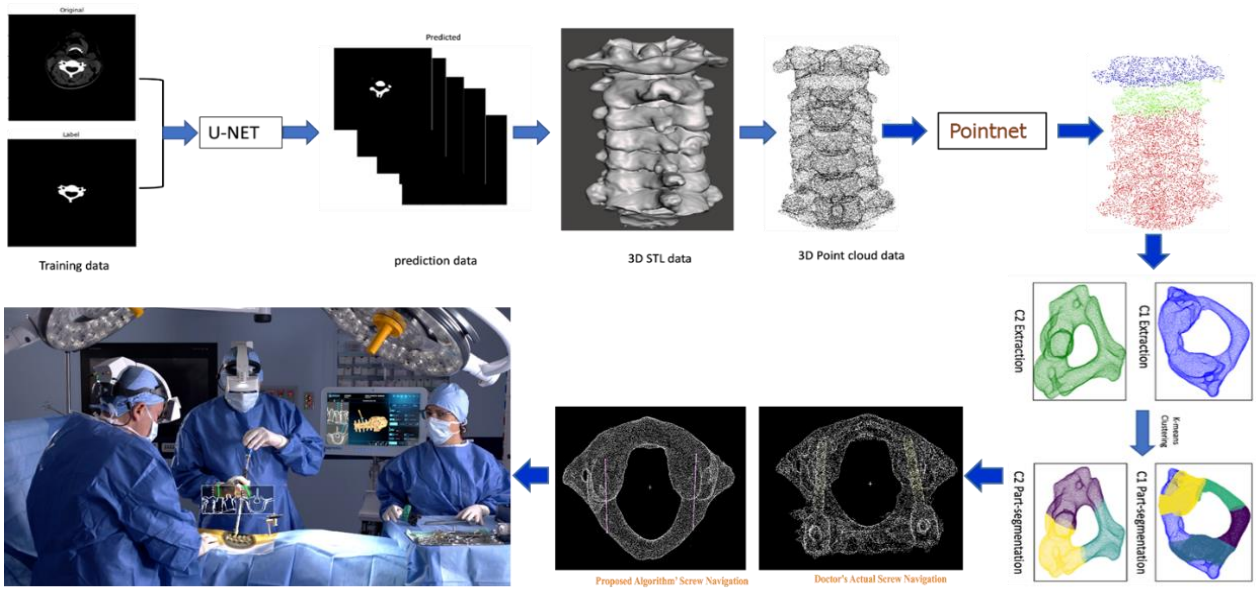


Fig. 23. Our proposed system. Start from the automatic path planning of pedicle screw placement to AR based 3D real-time cervical spine visualization and screw path surgical navigation

## 6. Expected Accomplishment and Requirements.

### 6.1 Expected Accomplishment of Work Items

**The first year:**

- Process 2D dicom images to reconstruct 3D mesh data
- Segment cervical spine by U-Net
- Convert 3D mesh to 3D point cloud data

- Cervical spine classification and part-segmentation into C1, C2 and C3-C7.
- C1 and C2 vertebrae segmentation into their anatomy using unsupervised learning.
- Develop an algorithm to obtained critical points in posterior arch, lamina, and lateral mass for screw navigation path.
- Pedicle screw placement path achieved using the critical points in C1 and C2 vertebrae.

**The second year:**

- Deep learning to find the pedicle screw placement path in automatic way.
- Ground truth data preparation to trained deep learning
- C1 and C2 vertebrae part-segmentation into critical regions using PointNet
- K-means clustering algorithm to obtained critical points for screw navigation path
- Pedicle screw placement path achieved using the critical points in C1 and C2 vertebrae.

**The third year:**

- Integration of first year and second year work into the augmented reality.
- Patients' information and DICOMM image registration in Hololens to interact with the patient spine in real time for surgery.
- Registration of Pedicle screw placement path achieved from first year and second year work in Hololens so that surgeons can perform the screw fixation surgery easily and safely.
- Improve the efficiency and accuracy of epipolar geometry algorithm so that surgeons can visualize the spine at any angle to ensure the safe of pedicle screw placement.

**6.2 Expected training**

The objective of this project is to learn and teach students about AI. Students will be involved and benefit from a close investigation of problems and the impact of the proposed solution on medical image analysis. Rigorous training for students is required to learn all the pros and cons of AI concepts. For this, we need to buy some required hardware and software for the project. Using the AR, the surgeons can interact with the patient's spine in real time and perform the pedicle screw placement using the navigation line obtained.

**6.3 Expected Research Results**

In the future, we will execute the proposed methods to design an automatic way to predict the pedicle screw navigation path in C1 and C2 and do a comparison with other ongoing research measures. Our objective is to first introduce the problem in a good conference paper and file for a patent. Based on the feedback we will intensify and diversify our proposed solutions and publish them in the SCI journal paper. Every year we are going to follow the same structure for our project.

**6.4 Expected Benefits for National Development and other Applications**

The research project will bring about the development of 3D medical images in Taiwan and improve the quality of current clinical preoperative manual planning and intraoperative surgery.

Therefore, the research will provide many options for Taiwan's new medical imaging industry, add value to the existing medical system, and ultimately bring new developments to the nation. In addition, the team is currently working with the French Poitiers University surgical robot team to bring new developments to international cooperation.

**Reference:**


[1] "Cervical Vertebrae - Physiopedia." https://www.physio-pedia.com/Cervical_Vertebrae.

[2] J.-T. Gräsner and L. Bossaert, "Epidemiology and management of cardiac arrest: What registries are revealing," *Best Practice & Research Clinical Anaesthesiology*, 2(3), pp. 293–306, 2013.

[3] F. M. Lomoschitz *et al.,* "Cervical spine injuries in patients 65 years old and older: epidemiologic analysis regarding the effects of age and injury mechanism on distribution, type, and stability of injuries," *AJR Am J Roentgenol*, 178(3), pp. 573–577, 2002.

[4] S. Bajada *et al.*, "Predictors of mortality following conservatively managed fractures of the odontoid in elderly patients," *Bone and Joint Journal*, 99(1), 116-121, 2017.

[5] T. Delcourt *et al.*, "Management of upper cervical spine fractures in elderly patients: current trends and outcomes," *Injury*, 46, pp. S24–S27, 2015.

[6] J. A. Menendez *et al.*, "Techniques of posterior C1-C2 stabilization," *Neurosurgery*, 60(1) SUPPL., 2007.

[7] R. J. Bransford *et al.*, "Posterior C2 instrumentation: Accuracy and complications associated with four techniques," *Spine (Phila Pa 1976)*, 36(14), 2011.

[8] M. Zarro *et al.*, Biomechanical comparison of the pullout strengths of C1 lateral mass screws and C1 posterior arch screws. *The Spine Journal*, 13(12), 1892-1896, 2013.

[9] Q.-Y. Zhou *et al.*, "Open3D: A Modern Library for 3D Data Processing," *arXiv preprint arXiv:1801.09847*, 2018.

[10] C. R. Qi *et al.*, "PointNet: Deep Learning on Point Sets for 3D Classification and Segmentation.", *IEEE/CVF Conference on Computer Vision and Pattern Recognition,* pp. 652–660, 2017.

[11] C. R. Qi *et al.*, "PointNet++: Deep Hierarchical Feature Learning on Point Sets in a Metric Space," *Adv Neural Inf Process Syst*, 30, 2017.

[12] M. Jaderberg *et al.*, "Spatial Transformer Networks," *Adv Neural Inf Process Syst*, vol. 28, 2015.

[13] R. Li et al., "Pointaugment: an auto-augmentation framework for point cloud classification." *IEEE/CVF Conference on Computer Vision and Pattern Recognition*, pp. 6378-6387, 2020.

[14] M. Eckert *et al.*„ "Augmented Reality in Medicine: Systematic and Bibliographic Review," *JMIR Mhealth Uhealth,* 7(4), p. e10967, 2019.

[15] J. Pottle, "Virtual reality and the transformation of medical education," *Future Healthc J*, 6(3), 2019.

[16] "Posterior C1-C2 fusion for C1-C2 Dislocation." *Spine*, 26(22), pp. 2467-2471, 2001.

[17] National Spinal Cord Injury Statistical Center, "Spinal cord injury facts and figures at a glance," *J Spinal Cord Med*, 36(1), pp. 1–2, 2013.

[18] "Cervical Spine Injury | Korey Stringer Institute." https://ksi.uconn.edu/emergency-conditions/cervical-spine-injury/.

[19] M. Song *et al.*, "Four lateral mass screw fixation techniques in lower cervical spine following laminectomy: A finite element analysis study of stress distribution," *Biomed Eng Online*, 13(1), 2014.

[20] "Lateral mass screw insertion (Magerl technique)." https://surgeryreference.aofoundation.org/spine/trauma/occipitocervical/basic-technique/lateral-mass-screw-insertion-magerl-technique.

[21] M. J. Lee *et al.*, "The feasibility of inserting atlas lateral mass screws via the posterior arch," *Spine (Phila Pa 1976)*, *31*(24), 2006.

[22] A. Eran *et al.*, "Asymmetry of the Odontoid Lateral Mass Interval in Pediatric Trauma CT: Do We Need to Investigate Further?," *American Journal of Neuroradiology*, 37(1), pp. 176–179, 2016.

[23] "CT scan – NHS," https://www.nhs.uk/conditions/ct-scan/.

[24] S. Targ *et al.*, "Resnet in Resnet: Generalizing Residual Architectures," *arXiv preprint arXiv:1603.08029*, 2016,

[25] J. Long, E. Shelhamer, and T. Darrell, "Fully Convolutional Networks for Semantic Segmentation." *IEEE conference on computer vision and pattern recognition,* pp. 3431–3440, 2015.

[26] O. Ronneberger *et al.*, "U-net: Convolutional networks for biomedical image segmentation," *Lecture Notes in Computer Science*, 9351, pp. 234–241, 2015.

[27] J. Wang *et al.*, "A Survey of 3D Image Navigation and High Precision Dynamic Registration in Minimally Invasive Surgery," *Procedia Comput Sci*, 131, pp. 320–326, 2018.

[28] M. Chen *et al.*, "The Application of Three-Dimensional Technology Combined With Image Navigation in Nasal Skull Base Surgery," *J Craniofac Surg*, *31*(8), Nov. 2020.
[29] R. Kochanski *et al.*, "Image-guided navigation and robotics in spine surgery," *Neurosurgery*, *84*(6), pp. 1179-1189, 2019.
[30] A. Arab *et al.*, "Use of 3D Navigation in Subaxial Cervical Spine Lateral Mass Screw Insertion," *J Neurol Surg Rep*, 79(1), pp. e1–e8, 2018.
[31] Z. Yu *et al.*, "Application of a novel 3D drill template for cervical pedicle screw tunnel design: a cadaveric study," *European Spine Journal*, 26(9), pp. 2348–2356, 2017.
[32] Y. Li *et al.*, "Comparative study of 3D printed navigation template-assisted atlantoaxial pedicle screws versus free-hand screws for type II odontoid fractures," *European Spine Journal*, 30(2), 2021.
[33] "Posterior C1–C2 Fusion With Polyaxial Screw and Rod Fixation: Spine," *Spine*, *26*(22), pp. 2467-2471, 2001.
[34] D. H. Lee *et al.*, "Optimal entry points and trajectories for cervical pedicle screw placement into subaxial cervical vertebrae," *European Spine Journal*, 20(6), pp. 905–911, 2011.
[35] D. M Sciubba et al., "Radiographic and clinical evaluation of free-hand placement of C-2 pedicle screws," *Journal of Neurosurgery: Spine*, 11(1), pp. 15-22, 2009.
[36] X. Qi et al., "An Automatic Path Planning Method of Pedicle Screw Placement Based on Preoperative CT Images," *IEEE Transactions on Medical Robotics and Bionics*, 4(2), pp. 403-413, 2022.
[37] D. Knez *et al.*, "Computer-assisted pedicle screw trajectory planning using CT-inferred bone density: A demonstration against surgical outcomes," *Medical Physics*, 46(8), pp. 3543–3554, 2019.
[38] W. Wi *et al.*., "Computed tomography-based preoperative simulation system for pedicle screw fixation in spinal surgery," *Journal of Korean Medical Science*, *35*(18), 2020.
[39] M. Soliman *et al.*, "Accuracy and efficiency of Fusion Robotics™ versus Mazor-X™ in single-level lumbar pedicle screw placement," *Cureus*, *13*(6), 2021.
[40] S. Caprara *et al.*, "Bone density optimized pedicle screw instrumentation improves screw pull-out force in lumbar vertebrae," *Taylor & Francis*, 25(4), pp. 464–474, 2021.
[41] L. Nolte *et al.*, "Clinical evaluation of a system for precision enhancement in spine surgery," *Clinical Biomechanics*, *10*(6), pp. 293-303, 1995.
[42] P. Park *et al.*, "Minimally invasive pedicle screw fixation utilizing O-arm fluoroscopy with computer-assisted navigation: Feasibility, technique, and preliminary results," *Surg Neurol Int*, 1(1), p. 44, 2010.
[43] A. Wolf *et al.*, "Feasibility study of a mini, bone-attached, robotic system for spinal operations: analysis and experiments," *Spine*, *29*(2), pp. 220-228, 2004.
[44] H. Kim *et al.*, "Monitoring the quality of robot-assisted pedicle screw fixation in the lumbar spine by using a cumulative summation test," *Spine,* 40(2), pp. 87-94, 2015.
[45] D. Devito *et al.*, "Clinical acceptance and accuracy assessment of spinal implants guided with SpineAssist surgical robot: retrospective study," *Spine*, *35*(24), pp. 2109-2115, 2010.
[46] X. Han *et al.*, "Safety and accuracy of robot-assisted versus fluoroscopy-assisted pedicle screw insertion in thoracolumbar spinal surgery: a prospective randomized controlled trial," *Journal of Neurosurgery: Spine*, *30*(5) , pp. 615-622, 2019.
[47] D. Gonzalez *et al.*, "Initial intraoperative experience with robotic-assisted pedicle screw placement with stealth navigation in pediatric spine deformity: an evaluation of the first 40 cases," *J Robot Surg*, *15*(5), pp. 687–693, 2021.
[48] H. Sumdani *et al.*, "Utility of augmented reality and virtual reality in spine surgery: a systematic review of the literature," *World neurosurgery*, *161*, e8-e17, 2022.
[49] G. Lee *et al.*, "What is your reality? Virtual, augmented, and mixed reality in plastic surgery training, education, and practice," *Plastic and Reconstructive Surgery*, 147(2), 2021
[50] A. Meola, F. Cutolo, M. Carbone, F. Cagnazzo, M. Ferrari, and V. Ferrari, "Augmented reality in neurosurgery: a systematic review," *Neurosurg Rev*, 40(4), pp. 537–548, 2017.
[51] P. E. Pelargos *et al.*, "Utilizing virtual and augmented reality for educational and clinical enhancements in neurosurgery," *Journal of Clinical Neuroscience*, 35, pp. 1–4, 2017.
[52] E. Watanabe *et al.*, "The Trans-Visible Navigator: A See-Through Neuronavigation System Using Augmented Reality," *World Neurosurg*, 87, pp. 399–405, 2016.
[53] G. Burström *et al.*, "Augmented and Virtual Reality Instrument Tracking for Minimally Invasive Spine Surgery: A Feasibility and Accuracy Study," *Spine (Phila Pa 1976)*, 44(15), pp. 1097–1104, 2019.
[54] F. Liebmann et al., "Pedicle screw navigation using surface digitization on the Microsoft HoloLens," *International journal of computer assisted radiology and surgery*, 14(7), pp. 1157-1165, 2019.
[55] R. Hartley et al., "Multiple View Geometry in computer vision. *Cambridge University Press*, 2003.